



Mechano-chemical synthesis of stoichiometric nickel and nickel-zinc ferrite powders with Nicolson-Ross analysis of the absorption coefficients

ČEDOMIR JOVALEKIĆ¹, ALEKSANDAR S. NIKOLIĆ^{2*}, MAJA GRUDEN-PAVLOVIĆ²
and MIODRAG B. PAVLOVIĆ³

¹Institute for Multidisciplinary Research, Kneza Višeslava 1a, 11001 Belgrade, Serbia,

²Faculty of Chemistry, Studentski trg 12–16, 11001 Belgrade, Serbia and ³Faculty of Electrical Engineering, B. Kralja Aleksandra 73, 11001 Belgrade, Serbia

(Received 2 March, revised 6 May 2011)

Abstract: The interest in finding new methods for the preparation of nickel ferrite (NiFe_2O_4) and nickel–zinc ferrite ($\text{Ni}_x\text{Zn}_{1-x}\text{Fe}_2\text{O}_4$) powders has recently increased, because the physical and chemical properties of these soft magnetic materials depend strongly on the preparation conditions. In this study, powder samples of ferrites were obtained by: 1) a classic sintering procedure ($\text{Ni}_x\text{Zn}_{1-x}\text{Fe}_2\text{O}_4$, $x = 0.9$) and 2) planetary mill synthesis (both NiFe_2O_4 and the $\text{Ni}_x\text{Zn}_{1-x}\text{Fe}_2\text{O}_4$). The mechano-chemical reaction leading to the formation of the spinel phase of $\text{Ni}_x\text{Zn}_{1-x}\text{Fe}_2\text{O}_4$ ($x = 1$ or 0.9) was monitored by scanning electron microscopy (SEM), transmission electron microscopy (TEM), and X-ray diffraction (XRD) analysis. The values of the real and imaginary parts of the permittivity and permeability were measured for the obtained nickel and nickel–zinc ferrite samples in the 7–12 GHz frequency range. Based on the obtained results, the electromagnetic radiation (EMR) absorption coefficients were calculated for all three types of sample. It was concluded that the method of preparation and the final particle size influence the EMR absorption coefficient of nickel and nickel–zinc ferrites.

Keywords: ferrites; nanocrystalline materials; mechano-chemistry; radar absorbers.

INTRODUCTION

It is well known that the properties of ferrite materials strongly depend on the preparation conditions. Consequently, different methods for the preparation of ferrite powders are described in the literature.^{1–3} By choosing a method that leads to a reduction of the particle size, the magnetic properties (such as coercive

*Corresponding author. E-mail: asn@chem.bg.ac.rs
doi: 10.2298/JSC110302186J

field, Curie temperature, saturation magnetization and absorption coefficients) may change significantly in comparison with those of the bulk material.

The basic structure of a spinel ferrite is $A_xB_{1-x}Fe_2O_4$, where A and B are divalent metal ions (*e.g.*, Mg, Mn, Ni, Zn, *etc.*). In a unit cell of the spinel lattice, there are eight tetrahedral and sixteen octahedral sites occupied by A, B and Fe^{3+} , while the oxygen anions are arranged in a cubic close-packed structure. Site occupancy may range from the normal spinel structure, in which the A and B cations occupy the tetrahedral sites and Fe^{3+} the octahedral ones, to the inverse spinel, in which half the Fe^{3+} cations occupy the tetrahedral sites, and three (A, B and Fe^{3+}) cations occupy the octahedral sites. In general, site occupancy in $NiFe_2O_4$ and $Ni_xZn_{1-x}Fe_2O_4$ may be expressed by rewriting its generic formula as $(Ni_{1-\lambda}Fe_\lambda)[NI_\lambda Fe_{1-\lambda}]O_4$ and $(Ni_xZn_{1-x})_{1-\lambda}Fe_\lambda][(Ni_xZn_{1-x})_\lambda Fe_{1-\lambda}]O_4$, where the parentheses and square brackets denote the tetrahedral and octahedral sites, respectively. λ represents the so-called degree of inversion, defined as the fraction of tetrahedral sites occupied by Fe^{3+} .

Interest in nanoparticle materials permanently increases because of the significant influence of large surface/volume ratio of nanoparticles on their physical properties, compared to their bulk counterpart.⁴ Recent investigations in the field of mechano-chemistry have resulted in the mechano-synthesis of stoichiometric and chemically pure nanoscale spinel ferrites,^{5–12} which were undertaken because this class of materials have significant permeability values over very narrow frequency ranges.^{13,14} In most cases, the complete formation of spinel ferrites was obtained only after milling followed by sintering, *i.e.*, by employing two processing steps. It was noted that the combined mechano-chemical-thermal treatment yielded a well-ordered spinel phase in ferrites at lower annealing temperatures and shorter durations, than those required for conventional ceramic methods.^{15,16} Herein, an improvement of the method in order to obtain ferrites with better properties, which can be employed in microwave electronics, is presented.

The request that an absorber of electromagnetic radiation (EMR) needs to be efficient can be satisfied by material with special properties. The material has to not only attenuate electromagnetic (EM) waves penetrating its volume, but also moreover present a good match to the incident waves at the air/material interface. Good absorption is provided with ϵ_r' , μ_r' , $\tan \delta_\mu$ and $\tan \delta_\epsilon$ as large as possible, while good matching at the interface requires $\mu_r' = \epsilon_r'$ and $\tan \delta_\mu = \tan \delta_\epsilon$.¹⁷ The present paper describes a technique for preparing nickel ferrite ($NiFe_2O_4$) and nickel-zinc ferrite ($Ni_{0.9}Zn_{0.1}Fe_2O_4$), based on planetary mill synthesis, which increases the absorption factor of ferrites obtained by the classical route, in the frequency range 7–12 GHz.^{18–21}

EXPERIMENTAL

Powder samples of NiFe_2O_4 and $\text{Ni}_{0.9}\text{Zn}_{0.1}\text{Fe}_2\text{O}_4$ soft ferrites were synthesized by classic sintering (sample **1** ($\text{Ni}_{0.9}\text{Zn}_{0.1}\text{Fe}_2\text{O}_4$), made in Ei Ferrite, Belgrade) and by planetary mill synthesis (sample **2** (NiFe_2O_4) and sample **3** ($\text{Ni}_{0.9}\text{Zn}_{0.1}\text{Fe}_2\text{O}_4$)).

In the classic sintering process, thermal diffusion occurs between NiO crystals (1–2 μm in size) and the hematite, and the final size of particles should be larger than the size of crystals in the starting components. The average particle size obtained by the conventional sintering method (sample **1**) was several microns.

Mixtures of crystalline powders of NiO and Fe_2O_3 for sample **2**, and NiO , ZnO and Fe_2O_3 (purity 99 %) for sample **3**, were used as the starting materials for the planetary mill syntheses. Mechano-chemical treatment was performed in a planetary ball mill (Fritsch Pulverisette 5). A hardened-steel vial (500 cm^3 volume) filled with 286 hardened-steel balls (8 mm in diameter) was used as the milling medium. The mass of the powders was 30 g and the balls-to-powder ratio was 20:1. Milling was performed for 50 h, in air, without any additives.

Sizes and shapes of polycrystalline powder particle of samples **2** and **3** were examined by scanning electron microscopy (SEM) (JEOL JSM-5200) and by combined field-emission (scanning) transmission electron microscopy (TEM) (the grid was dried overnight at room temperature and observed with a FEI Tecnai biotwin (120 kV)) and by X-ray diffraction (XRD) analysis. Prior to the SEM surveys, the particles were gold-sputtered in a JFC 1100 ionic sputter coater. Prior to the TEM investigations, the powders were crushed in a mortar, dispersed in ethanol and fixed on a copper-supported carbon film. The XRD analysis of samples **2** and **3** was performed on a Philips PW 1730 automatic diffractometer with CuK_α graphite-monochrome radiation ($\lambda = 0.1542 \text{ nm}$).

Values of the real and imaginary parts of the permittivity and permeability were measured for all three samples in the 7–12 GHz frequency range. Samples were prepared by pressing the powder into aluminum holders (27 mm×27 mm) without thermal treatment. The measurements were performed using a HP 8510 network analyzer system with simple-to-fabricate test fixtures, with the capability to measure simultaneously both μ_r and ϵ_r at up to 400 frequency points. Based on the values obtained for μ_r and ϵ_r , the EMR absorption coefficient was calculated.

RESULTS AND DISCUSSION

SEM Micrographs of powder samples of NiFe_2O_4 (sample **2**) and $\text{Ni}_{0.9}\text{Zn}_{0.1}\text{Fe}_2\text{O}_4$ (sample **3**) synthesized by the planetary mill procedure are shown in Fig. 1. It can be noticed that the nanoscale crystallites tend to agglomerate, because of the dipolar field of each crystallite. TEM Micrographs of samples **2** and **3**, presented in Fig. 2, show that the nanoscale crystallites form particles of average size 10–15 nm, which is consistent with the average crystallite size determined by XRD analysis. The shape of the majority of the crystallites appears to be spherical. Agglomerated crystallites form particles with sizes mostly up to 50 nm.

The X-ray diffractograms of samples **2** and **3** are presented in Fig. 3. They show that no peaks of the starting compounds were present after 50 h of milling, only the full spectrum of the characteristic peaks of NiFe_2O_4 in sample **2** and those of $\text{Ni}_{0.9}\text{Zn}_{0.1}\text{Fe}_2\text{O}_4$ in sample **3**. The calculated lattice parameters were

0.83369 ± 10^{-5} for NiFe_2O_4 and 0.83401 ± 10^{-5} nm for $\text{Ni}_{0.9}\text{Zn}_{0.1}\text{Fe}_2\text{O}_4$, which are consistent with the values obtained by other authors (ICPD 10-325; ICPD 22-1012).

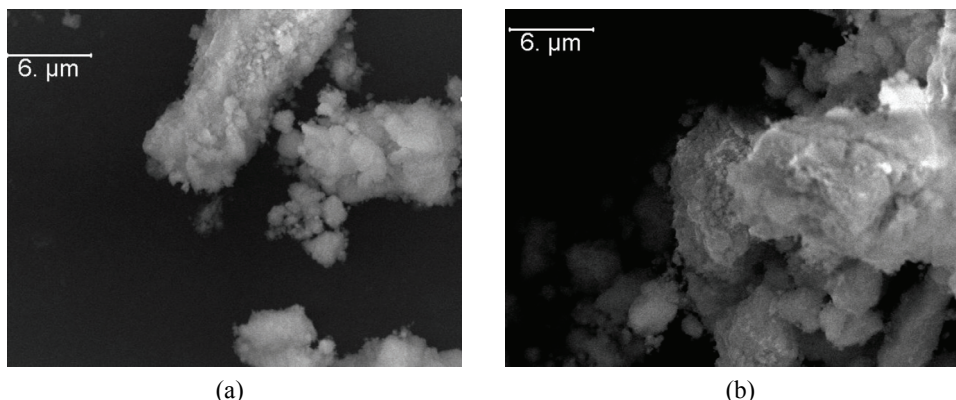


Fig. 1. SEM Images of the nanocrystalline mechano-synthesized samples after 50 h of milling:
a) sample 2 (NiFe_2O_4) and b) sample 3 ($\text{Ni}_{0.9}\text{Zn}_{0.1}\text{Fe}_2\text{O}_4$).

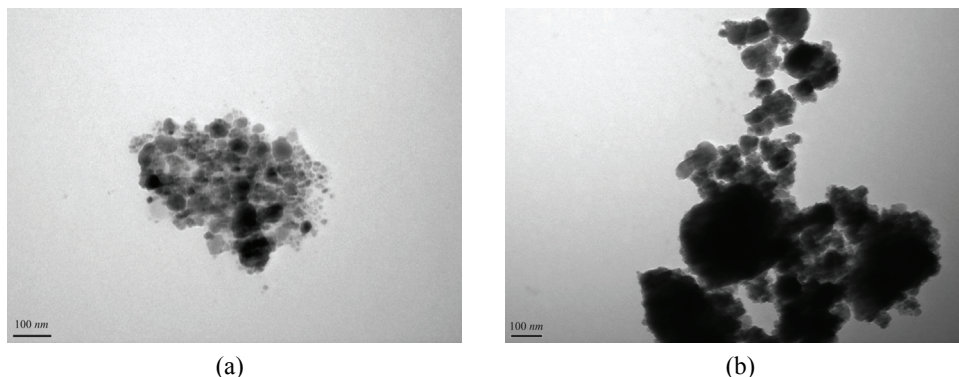


Fig. 2. TEM Images of the nanocrystalline mechano-synthesized samples after 50 h of milling: a) sample 2 (NiFe_2O_4) and b) sample 3 ($\text{Ni}_{0.9}\text{Zn}_{0.1}\text{Fe}_2\text{O}_4$).

Crystallite sizes of the powders were calculated from the XRD data by means of the Scherrer Equation:²²

$$S = \frac{0.9\lambda}{B \cos \theta_B} \quad (1)$$

where S is the crystallite grain size, λ is the wavelength of the X-ray source, θ_B is the Bragg angle of the considered XRD peaks, and B represents the full width at half maximum (FWHM) line broadening obtained as follows:

$$B^2 = B_m^2 - B_s^2 \quad (2)$$

where B_m is the FWHM line broadening of the material and B_s represents the FWHM line broadening of the internal standard (α -Al₂O₃). The resulting values of crystallite size obtained from the strongest (111) reflections were in the range of 10–15 nm for NiFe₂O₄ and Ni_{0.9}Zn_{0.1}Fe₂O₄.

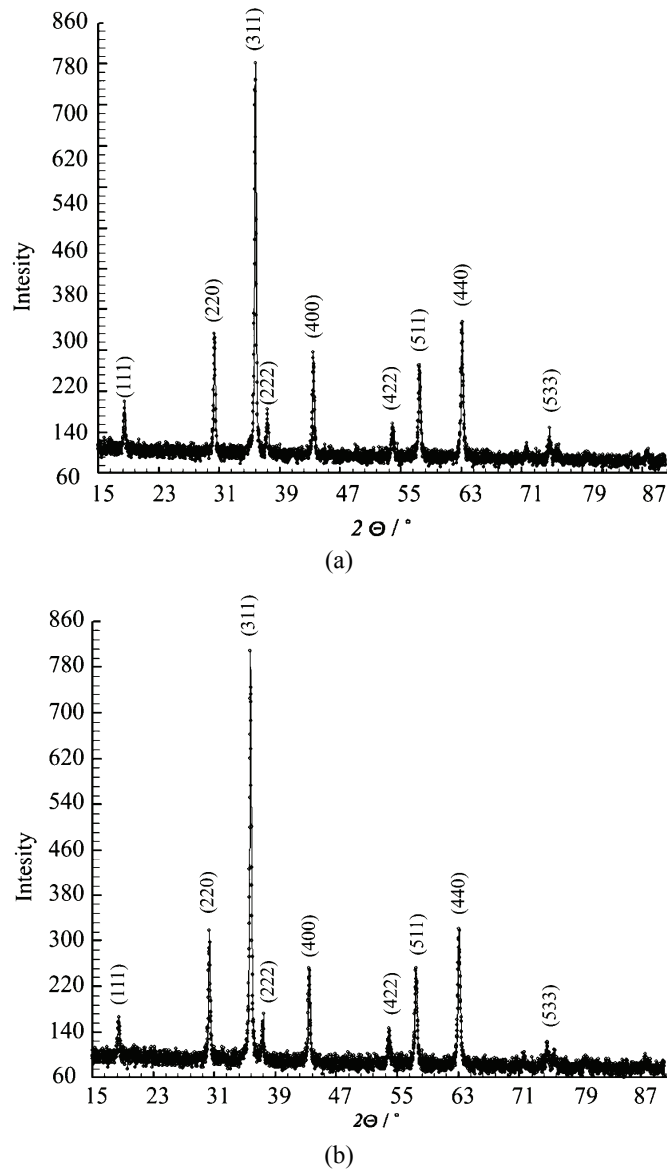


Fig. 3. XRD Patterns of the mechano-synthesized samples after 50 h of milling:
a) sample 2 (NiFe₂O₄) and b) sample 3 (Ni_{0.9}Zn_{0.1}Fe₂O₄).

The complex permittivity and permeability values of all ferrite samples were obtained from measurements conducted using an HP 8510 Network Analyzer system. From the obtained frequency dependence of the permittivity and permeability, the EMR attenuation coefficient α was calculated using the formula:

$$\alpha = 2\pi f \sqrt{\mu_0 \epsilon_0} \sqrt{\epsilon_r' \mu_r' / 2} \times \\ \times \sqrt{(\tan \delta_\mu \tan \delta_\epsilon - 1) + (1 + \tan^2 \delta_\mu \tan^2 \delta_\epsilon + \tan^2 \delta_\mu + \tan^2 \delta_\epsilon)^{1/2}} \quad (3)$$

where the loss tangents are defined by $\tan \delta_\mu = \mu_r''/\mu_r'$ and $\tan \delta_\epsilon = \epsilon_r''/\epsilon_r'$ (μ_r' and ϵ_r' being the real parts, and μ_r'' and ϵ_r'' the imaginary parts of the permeability and permittivity, respectively).

The real and complex parts of the permittivity exhibited frequency dependency in all three samples, but without any marked maximum values; hence all the examined materials could be used as wide-range absorbents. Samples **1** and **3** exhibited higher values of the real part of the permittivity than those of sample **2**. Conversely, sample **2** exhibited higher values of the imaginary part of the permittivity than the other two sample types (Fig. 4). The real part of the permeability was the highest in sample **3**, and the lowest in sample **2**. Sample **1** and sample **2** exhibited higher values of the imaginary part of permeability than those of sample **3** (Fig. 5).

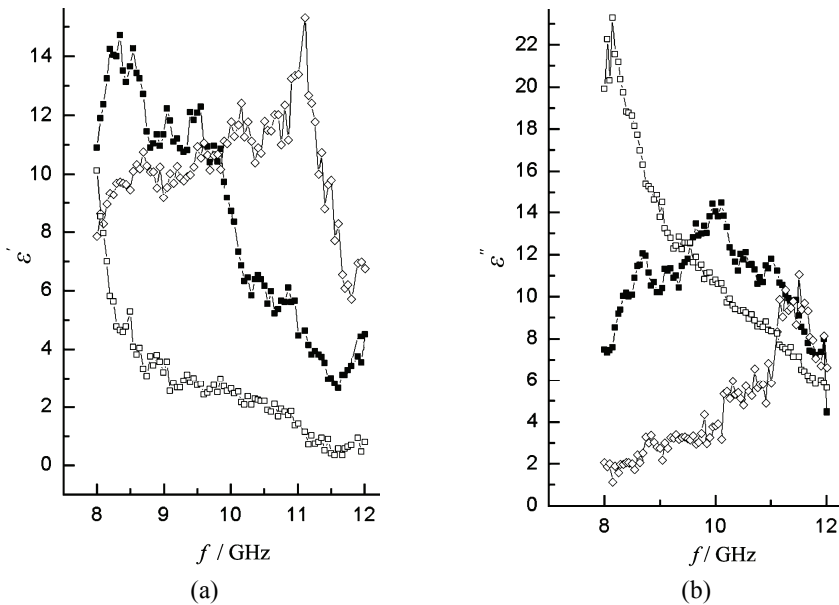


Fig. 4. Values of the real, ϵ_r' (a), and the imaginary part, ϵ_r'' (b), of permittivity for the ferrite samples: \diamond – $\text{Ni}_{0.1}\text{Zn}_{0.9}\text{Fe}_2\text{O}_4$ (sample **1**) obtained by the standard sintering route, \square – NiFe_2O_4 (sample **2**) and \blacksquare – $\text{Ni}_{0.1}\text{Zn}_{0.9}\text{Fe}_2\text{O}_4$ (sample **3**) obtained mechano-chemically.

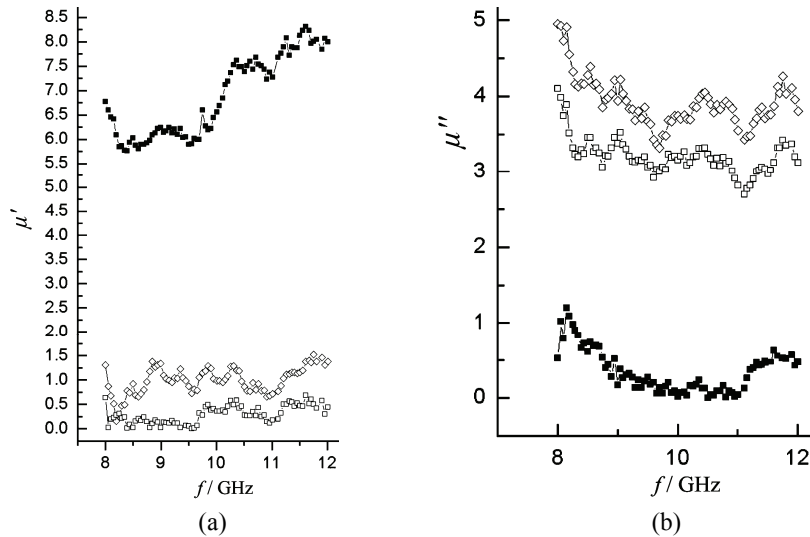


Fig. 5. Values of the real, μ'_r (a), and the imaginary part, μ''_r (b), of permeability for ferrite samples: \diamond – $\text{Ni}_{0.1}\text{Zn}_{0.9}\text{Fe}_2\text{O}_4$ (sample 1) obtained by the standard sintering route, \square – NiFe_2O_4 (sample 2) and \blacksquare – $\text{Ni}_{0.1}\text{Zn}_{0.9}\text{Fe}_2\text{O}_4$ (sample 3) obtained mechano-chemically.

The values of the EMR attenuation coefficient (α) calculated from expression (3) are presented in Fig. 6, in linear and log scales. It may be concluded that the EMR attenuation coefficient depended more on the method of preparation,

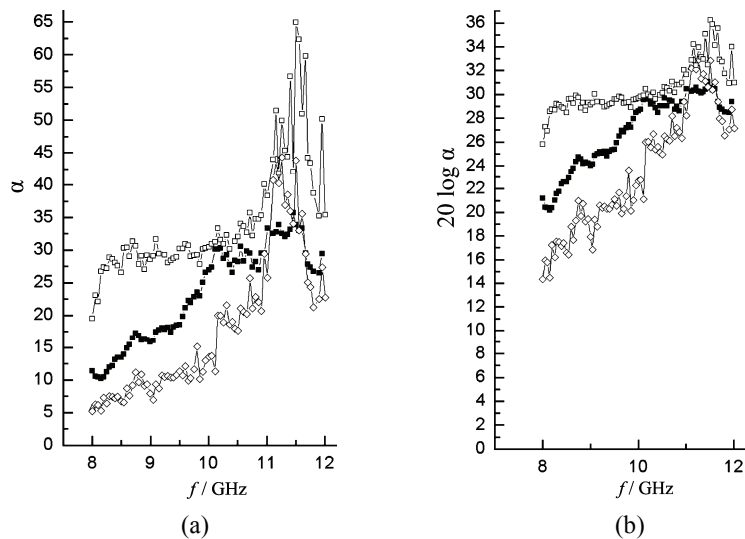


Fig. 6. Values of EMR attenuation coefficient (α) for \diamond – $\text{Ni}_{0.1}\text{Zn}_{0.9}\text{Fe}_2\text{O}_4$ (sample 1) obtained by the standard sintering route, \square – NiFe_2O_4 (sample 2) and \blacksquare – $\text{Ni}_{0.1}\text{Zn}_{0.9}\text{Fe}_2\text{O}_4$ (sample 3), presented in a) linear and b) logarithmic scale.

i.e., on powder particle morphology than on the chemical content of the samples. It can be seen in Figure 6b that the change of attenuation coefficient for sample **2** was within 30 dB, for sample **3** between 20 and 30 dB, and for sample **1** between 10 and 30 dB. The higher values of the EMR attenuation coefficient observed for samples **2** and **3**, obtained by the mechano-chemical process, are the result of the extremely high specific granule surface (granule-weight to granule-surface ratio), as well as of the large number of dislocations and impurities in the crystal structure concentrated at the granule surfaces, which is typical for powders obtained mechano-chemically. Larger granules present in sample **1** resulted in lower values of the EMR attenuation coefficient.

CONCLUSION

Based on the obtained results, it can be concluded that the nickel ferrite (NiFe_2O_4) produced by the mechano-chemical process gave better results with respect to EMR attenuation than the nickel–zinc ferrite obtained by both the classic and mechano-chemical sintering process. For the mechano-chemically prepared nickel ferrite samples, the EMR attenuation coefficient showed a practically constant value (within a 30 dB margin) over the whole frequency range (7–12 GHz), which places these soft ferrites among the most favorable wide-range microwave absorbents. The configuration of the soft ferrites obtained by this method is a single-layer one, as opposed to the complex multi-layer configurations applied hitherto. Final judgment on the applicability of these materials for wide-range radar absorbers demands an extension of this investigation toward higher frequencies.

Acknowledgements. The Ministry of Education and Science of the Republic of Serbia supported this work.

ИЗВОД

МЕХАНОХЕМИЈСКА СИНТЕЗА НИКАЛ И НИКАЛ–ЦИНК ФЕРИТНИХ ПРАХОВА СА
NICOLSON–ROSS АНАЛИЗОМ АБСОРПЦИОНИХ КОЕФИЦИЈЕНТА

ЧЕДОМИР ЈОВАЛЕКИЋ¹, АЛЕКСАНДАР С. НИКОЛИЋ², МАЈА ГРУДЕН-ПАВЛОВИЋ²
и МИОДРАГ Б. ПАВЛОВИЋ³

¹Институут за мултидисциплинарна истраживања, Кнеза Вишеслава 1а, 11001 Београд, ²Хемијски
факултет, Студентски трг 12–16, 11001 Београд и ³Електротехнички факултет,
Б. Краља Александра 73, 11001 Београд

У новије време повећан је интерес за проналажење нових метода за синтезу никал-ферита (NiFe_2O_4) и никал–цинк-феритних ($\text{Ni}_x\text{Zn}_{1-x}\text{Fe}_2\text{O}_4$) прахова, због чињенице да физичка и хемијска својства ових „меких“ магнетних материјала у многоме зависе од услова припреме. Добијени феритни прахови, описани у овом раду, синтетисани су: 1) класичном процедуром синтеровања ($\text{Ni}_x\text{Zn}_{1-x}\text{Fe}_2\text{O}_4$, $x = 0,9$ или 2) синтезом у планетарном млину (NiFe_2O_4 и $\text{Ni}_x\text{Zn}_{1-x}\text{Fe}_2\text{O}_4$). Просечна величина честица добијених првом методом износи 3–5 μm, док друга метода даје честице величине 10–12 nm. Карактеризација узорака праћена је скенирајућом електронском микроскопијом (SEM), трансмисионом електронском микро-

скопијом (TEM), као и дифракционом анализом X-зрацима (XRD). Реални и имагинарни делови коефицијената пермитивности и пермеабилности су мерени на добијеним узорцима никал и никал–цинк-ферита у фреквентном опсегу 7–12 GHz . На основу добијених резултата, израчунати су EMR апсорпциони коефицијенти за све добијене узорке. Закључено је да је начин припреме, као и добијена величина честица, утичу на EMR апсорпционе коефицијенте никал и никал–цинк-ферита.

(Примљено 2. марта, ревидирано 6. маја 2011)

REFERENCES

1. W. C. Kim, S. J. Kim, C. S. Kim, *J. Appl. Phys.* **91** (2002) 7607
2. C. Huang, E. Matijevic, *Solid State Ionics* **84** (1996) 249
3. A. Anwar, T. Fujiwara, S. Song, M. Yoshimura, *Solid State Ionics* **151** (2002) 419
4. F. Vetrone, J.-C. Boyer, J. A. Capobianco, A. Speghini, M. Bettinelli, *Nanotechnology* **15** (2004) 75
5. E. Manova, B. Kunev, D. Paneva, I. Mitov, L. Petrov, C. Estournes, C. D. Orleans, J.-L. Rehspringer, M. Kurmoo, *Chem. Mater.* **16** (2004) 5689
6. M. Muroi, R. Street, P. McCormick, G. Amighian, *J. Phys. Rev. B* **63** (2001) 184414
7. P. Druska, U. Steinike, V. Šepelak, *J. Solid State Chem.* **13** (1999) 146
8. V. Šepelak, S. Wissmann, K. D. Becker, *J. Magn. Magn. Mater.* **203** (1999) 135
9. V. G. Harris, D. J. Fatemi, J. O. Cross, E. E. Carpenter, V. M. Browning, J. P. Kirkland, A. Mohan, G. J. Long, *J. Appl. Phys.* **94** (2003) 496
10. R. N. Bhowmik, R. Ranganathan, *J. Mater. Sci.* **37** (2002) 4391
11. N. Guigue-Millot, S. Begin-Colin, Y. Champion, M. J. Hytch, G. Le Caer, P. Perriat, *J. Solid State Chem.* **170** (2003) 30
12. V. Šepelak, M. Menzel, I. Bergmann, M. Wiebcke, F. Krumeich, K. D. Becker, *J. Magn. Magn. Mater.* **1616** (2004) 272
13. H. Severin, P. J. Stoll, *Z. Angew. Phys.* **23** (1967) 209
14. B. Heck, *Magnetic Materials and their Applications*, Butterworths, London, UK, 1974
15. H. M. Yang, X. C. Zhang, A. D. Tang, G. Z. Qiu, *Chem. Lett.* **33** (2004) 826
16. G. Ennas, G. Marongiu, S. Marras, G. Piccaluga, *J. Nanopart. Res.* **6** (2004) 99
17. I. Nicolaescu, *J. Optoelectron. Adv. Mater.* **8** (2006) 333
18. Č. Jovalekić, M. Zdujić, A. Radaković, M. Mitić, *Mat. Lett.* **24** (1995) 365
19. M. Zdujić, Č. Jovalekić, Lj. Karanović, M. Mitić, D. Poleti, D. Skala, *Mater. Sci. Eng., A* **245** (1998) 109
20. M. Zdujić, Č. Jovalekić, Lj. Karanović, M. Mitić, *Mater. Sci. Eng., A* **266** (1999) 204
21. A. S. Nikolić, P. Osmoković, D. Manojlović, N. Šojić, M. B. Pavlović, *J. Optoelectron. Adv. Mater.* **10** (2008) 1390
22. B. E. Warren, *X-Ray Diffraction*, Addison-Wesley, Reading, MA, USA, 1969.

